ISSN 1070-3284, Russian Journal of Coordination Chemistry, 2014, Vol. 40, No. 9, pp. 676–685. © Pleiades Publishing, Ltd., 2014.

Three One-Dimensional Chains with Bulky Backbone Carboxylate Ligands: Syntheses, Crystal Structures, and Luminescent Properties[1]

J. J. Wang[a], *, Y. H. Guo[b], Y. T. Wang[a], and T. Y. Wang[a]

[a]*College of Chemistry and Chemical Engineering, Anyang Normol University, Anyang, Henan, 455000 P.R. China*

[b]*College of Chemistry and Environmental Engineering, Anyang Institute of Technology, Anyang, Henan, 455000 P.R. China*

**e-mail: jjwang@aynu.edu.cn*

Received March 2, 2014

Abstract—To explore the influence of bulky backbone on complexes, three Co(II) and Zn(II) complexes with phenanthrene-9-carboxylate (L^1), 9*H*-fluorene-9-carboxylate (L^2) or biphenyl-4-carboxylate (L^3) together with incorporating auxiliary bridging ligad 4,4'-bipyridine (4Bipy), were synthesized and characterized: $[Co(L^1)_2(4Bipy)(H_2O)_2]_\infty$ (**I**), $[Zn(L^2)_2(4Bipy)_{0.5}(4Bipy)_{0.5}]_\infty$ (**II**), and $[Zn_3(L^3)_4(4Bipy)_{0.5}(4Bipy)_{0.5}(4Bipy)_{0.5}(OH)_2]_\infty$ (III). X-ray single-crystal diffraction analyses show that complexes **I**–**III** both assume one-dimensional (1D) structures by incorporating the bridging 4Bipy (CIF file CCDC nos. 942729 (**I**), 942727 (**II**), and 942733 **III**). In **I**, mononuclear six-coordinated Co^{2+} ions are linked into a 1D linear chain by 4Bipy. While in **II**, mononuclear four-coordinated Zn^{2+} ions are linked into a 1D zigzag chain by 4Bipy. But in **III**, because of the existence of OH^-, hexanuclear Zn(II) can be regarded as a node, then bridge adjacent hexanuclear Zn(II) nodes by almost parallelled three 4Bipy ligands into a 1D linear chain. Finally the 1D chains of **I**–**III** are further assembled into an overall three-dimensional (3D) framework via intermolecular H-bonding, π···π stacking, and/or C–H···π supramolecular interactions, respectively. The results indicate that, besides different metal ions Co^{2+} and Zn^{2+} or OH^- anions, the steric hindrance of backbone ligands play an important role in the formation of **I**–**III**. Moreover, the luminescent properties of corresponding ligands and their complexes were briefly investigated.

DOI: 10.1134/S1070328414090127

INTRODUCTION

There is currently considerable interest in the design and synthesis of metal polymers due to not only their intriguing structural diversity but also their potential applications in molecular adsorption and separation processes, gas storage, ion exchange, catalysis, sensor technology and so on [1–4]. In this field, the choice of suitable organic ligands favoring structure-specific self-assembly is crucial for the construction of prospective coordination structures with relevant properties and functions [5–8]. Among various ligands, the versatile carboxylic acid ligands, especially bulky backbone multi-carboxylic acid ligands, such as naphthalene-1,4-dicarboxylic acid [9–12], naphthalene-1,5-dicarboxylic acid [13], naphthalene-2,6-dicarboxylic acid [14–18], anthracene-9,10-dicarboxylic acid [19–21] and anthracene-1,5-dicarboxylic acid [21], have been well used in the preparation of various metal complexes owing to their rich coordination modes. In contrast, in this regard, the skillful use of monocarboxylic acid ligands with bulky backbone to construct functional metal compounds has been less investigated to date. Bulky backbone, as an important part of the ligand, as well as auxiliary ligands, counteranions, the pH values of the reaction solutions, temperature, molar ratio between reactants, and solvent system [22, 23], can not only play an important role in the formation of complexes, but also can exert a deciding influence on their structures and functions (or properties).

In our previous work, four monocarboxylate bulky backbone ligands, anthracene-9-carboxylic acid [24], phenanthrene-9-carboxylic acid [25], 2-phenylquinoline-4-carboxylic acid [25] and adamantane-1-carboxylic acid [25], had been successfully used to construct the Ag(I), Cu(II), Co(II), Ni(II), Mn(II), and Cd(II) complexes, which exhibited interesting magnetic and luminescent properties. Considering all the aspects stated above, we select three representative ligands with different bulky substituent backbones, phenanthrene-9-carboxylic acid (HL^1), 9*H*-fluorene-9-carboxylic acid (HL^2) and biphenyl-4-carboxylic acid (HL^3) together with incorporating auxiliary bridging ligand 4,4'-bipyridine (4Bipy), to construct corresponding Co(II) and Zn(II) coordination polymers: $[Co(L^1)_2(4Bipy)(H_2O)_2]_\infty$ (**I**), $[Zn(L^2)_2(4Bipy)_{0.5}(4Bipy)_{0.5}]_\infty$ (**II**) and $[Zn_3(L^3)_4(4Bipy)_{0.5}(4Bipy)_{0.5}(4Bipy)_{0.5}(OH)_2]_\infty$ (**III**).

[1] The article is published in the original.

Furthermore, the luminescent properties of the corresponding complexes and ligands in the solid state at room temperature have been investigated.

EXPERIMENTAL

Materials and methods. Ligand HL^1 was synthesized according to literature procedure [26], and all the other reagents and solvents for synthesis were commercially available and used as received or purified by standard methods prior to use. Elemental analyses (C, H, and N) were performed on a PerkinElmer 240C analyzer. The IR spectra were recorded in the range 4000–400 cm^{-1} on a Tensor 27 OPUS (Bruker) FT-IR spectrometer with KBr pellets. The emission/excitation spectra were recorded on a Cary Eclips fluorescence spectrophotometer. The X-ray powder diffraction patterns (XRPD) were recorded on a Rigaku D/Max-2500 diffractometer, operated at 40 kV and 100 mA, using a Cu-target tube and a graphite monochromator. The intensity data were recorded by continuous scan in a $2\theta/\theta$ mode from 3° to 35° with a step size of 0.02° and a scan speed of 8° min^{-1}.

Synthesis of I. An ethanol solution (10 mL) containing HL^1 (0.1 mmol), 4Bipy (0.05 mmol) and excess 2,6-dimethylpyridine (~0.05 mL for adjusting the pH value) was carefully layered on top of an aqua solution (15 mL) of $Co(ClO_4)_2 \cdot 6H_2O$ (0.05 mmol) in a test tube. Red single crystals suitable for X-ray analysis appeared at the boundary between two layers of solutions after *ca*. one month at room temperature. The yield was ~20% based on HL^1.

IR (KBr; ν, cm^{-1}): 3450 s, br., 2096 w, 1598 s, 1550 s, 1416 s, 1308 w, 1160 w, 1068 m, 1029 w, 956 w, 909 w, 875 w, 846 m, 819 w, 794 w, 752 m, 708 s, 682 m, 630 m, 523 m.

For $C_{40}H_{30}N_2O_6Co$			
anal. calcd., %:	C, 69.25;	H, 4.36;	N, 4.04.
Found, %:	C, 68.95;	H, 4.45;	N, 4.37.

Synthesis of II. The same procedure as that for **I** was used for this complex except that $Co(ClO_4)_2 \cdot 6H_2O$ and HL^1 were replaced by $Zn(Ac)_2 \cdot 2H_2O$ and HL^2. Yellow single crystals suitable for X-ray analysis appeared at the tube wall after ca. one month at room temperature. The yield was ~30% based on HL^2.

IR (KBr; ν, cm^{-1}): 3355 s, br., 2101 w, 1601 s, 1557 s, 1420 s, 1312 w, 1161 w, 1065 m, 1032 w, 1003 w, 950 w, 906 w, 879 m, 843 w, 815 w, 792 w, 786 w, 757 m, 701 s, 684 s, 638 m, 529 m.

For $C_{38}H_{26}N_2O_4Zn$			
anal. calcd., %:	C, 71.46;	H, 4.11;	N, 4.39.
Found., %:	C, 71.69;	H, 4.38;	N, 4.05.

Synthesis of III. The same procedure as that for **II** was used for this complex except that HL^2 and 2,6-dimethylpyridine were replaced by HL^3 and NaOH. Yellow single crystals suitable for X-ray analysis appeared at the tube wall after *ca*. one month at room temperature. The yield was ~20% based on HL^3.

IR (KBr; ν, cm^{-1}): 3318 s, br., 2748 w, 1623 m, 1597 s, 1577 s, 1486 w, 1448 w, 1395 s, 1362 m, 1226 w, 1102 w, 1007 w, 866 w, 809 m, 751 s, 693 m, 633 m, 543 w, 480 m.

For $C_{67}H_{50}N_3O_{10}Zn_3$			
anal. calcd., %:	C, 64.42;	H, 4.04;	N, 3.37.
Found, %:	C, 64.07;	H, 4.45;	N, 3.58.

XRPD patterns of **I**–**III** were recorded at 293 K on a Rigaku D/Max-2500 diffractometer, operated at 40 kV and 100 mA, using a Cu-target tube and a graphite monochromator. The crushed single-crystalline powder samples were prepared by crushing the crystals and the intensity data were recorded by continuous scan in the $2\theta/\theta$ mode from 3° to 35° with a step size of 0.02° and a scan speed of 8° min^{-1}. Simulation of the XRPD spectra was carried out by the single-crystal data and diffraction-crystal module of the Mercury (Hg) program available free of charge via the internet at http://www.iucr.org.

X-ray crystallography. Single-crystal X-ray single-crystal diffraction measurement for complexes I and **II** were carried out on a Rigaku SCX-mini diffractometer and a Bruker Smart 1000 CCD diffractometer equipped with a graphite crystal monochromator situated in the incident beam for data collection at 293(2) and 294(2) K, respectively. The determinations of unit cell parameters and data collections were performed with MoK_α radiation (λ = 0.71073 Å) and unit cell dimensions were obtained with least-square refinements. The program SAINT [27] was used for integration of the diffraction profiles. Semi-empirical absorption corrections were applied using SADABS program [28]. All the structures were solved by direct methods using the SHELXS program of the SHELXTL package and refined with SHELXL [29]. Metal atoms in each complex were located from the *E*-maps, and other non-hydrogen atoms were located in successive difference Fourier syntheses and refined with anisotropic thermal parameters on F^2. The hydrogen atoms were added theoretically, riding on the concerned atoms and refined with fixed thermal factors. Crystallographic data and experimental details for structural analyses are summarized in Table 1. Selected bond distances and angles are listed in Table 2.

Supplementary material for structures **I**–**III** has been deposited with the Cambridge Crystallographic Data Centre (nos. 942729, 942727, and 942733, respectively; deposit@ccdc.cam.ac.uk or http://www.ccdc.cam.ac.uk).

Table 1. Crystallographic data and structure refinement summary for compounds **I–III**

Parameter	Value		
	I	**III**	**II**
Formula weight	1387.18	639.98	1253.21
Crystal system	Orthorhombic	Monoclinic	Monoclinic
Space group	*Pbcn*	*Cc*	$P2_1/c$
a, Å	27.632(6)	10.983(7)	18.173(4)
b, Å	11.441(2)	14.913(10)	14.091(3)
c, Å	10.047(2)	17.827(11)	21.977(4)
β, deg	90	96.627(11)	97.58(3)
V, Å^3	3176.4(11)	2900(3)	5578.6(19)
Z	4	4	4
ρ_{calcd}, g cm^{-3}	1.450	1.466	1.492
μ, mm^{-1}	0.595	0.894	1.346
T, K	293(2)	294(2)	293(2)
θ Range, deg	1.93–25.01	2.31–26.46	3.04–25.01
Index range *h*, *k*, *l*	$-32 \le h \le 32$, $-13 \le k \le 13$, $-11 \le l \le 11$	$-7 \le h \le 13$, $-18 \le k \le 18$, $-22 \le l \le 13$	$-21 \le h \le 21$, $-16 \le k \le 16$, $-26 \le l \le 26$
Measured reflections	22163	6742	46031
Independent reflections	2796	3515	9817
R_{int}	0.0710	0.0533	0.0901
Observed reflections	232	406	748
GOOF	1.229	0.943	1.120
$R/wR^*(I > 2\sigma(I))$	0.0554/0.1154	0.0399/0.0664	0.0636/0.0948
R/wR^*(all data)	0.0572/0.1163	0.0653/0.0736	0.0989/0.1045
$\Delta\rho_{max}/\Delta\rho_{min}$, *e* Å^{-3}	0.256/–0.379	0.289/–0.393	0.353/–0.368

$^*R = \Sigma(\|F_0\| - |F_c\|)/\Sigma|F_0|$; $wR = [\Sigma w(|F_0|^2 - |F_c|^2)^2/\Sigma w(F_0^2)]^{1/2}$.

RESULTS AND DISCUSSION

Generally, properly lowering the reaction speed may result in the formation of crystalline products to facilitate the slow growth of well-shaped larger single crystals suitable for X-ray diffraction [30]. Considering this point, the synthesis and isolation of **I–III** in this research were carried out through self-assembly reaction of $Co(ClO_4)_2 \cdot 6H_2O$ or $Zn(Ac)_2 \cdot 2H_2O$ with HL^1, HL^2 or HL^3, together with introducing 4Bipy as a bridging co-ligand, by using the slow diffusion method in a test tube under mild conditions of ambient temperature and pressure.

Complexes **I–III** are all air stable. All general characterizations were carried out with crystal samples. As such, the elemental analyses of **I–III** are also consistent with the results of their structural analysis. In general, the IR spectra show features attributable to each component of the complexes [31]. The characteristic bands of carboxylate groups appeared in the usual region at 1601–1550 cm^{-1} for the antisymmetric stretching vibrations and at 1420–1395 cm^{-1} for the symmetric stretching vibrations, in good agreement with their solid structural features from the results of crystal structures [31, 32].

As shown in Fig. 1a, each asymmetric unit of **I** is composed of half Co^{2+} ions, one L^1 ligands, half 4Bipy ligands and one coordinated aqua molecule. Each Co^{2+} ion is six-coordinated by two carboxylate O atoms from two different L^1 ligands in monodentate coordination mode, two N atoms from two 4Bipy

Table 2. Selected bond lengths (Å) and angles (deg) for compound **I**–**III***

Bond	*d*, Å	Bond	*d*, Å
	I		
Co(1)–O(2)	2.112(2)	Co(1)–O(3)	2.125(2)
Co(1)–N(1)$^{\#2}$	2.136(4)	Co(1)–N(2)	2.196(4)
	II		
Zn(1)–O(1)	1.927(4)	Zn(1)–O(3)	1.937(3)
Zn(1)–N(2)	2.040(5)	Zn(1)–N(1)	2.072(5)
	III		
Zn(1)–O(10)$^{\#1}$	1.927(3)	Zn(1)–O(6)$^{\#1}$	1.966(3)
Zn(1)–O(9)	1.982(3)	Zn(1)–N(1)	2.146(3)
Zn(1)–O(10)	2.247(3)	Zn(2)–O(10)	2.055(3)
Zn(2)–O(7)	2.077(3)	Zn(2)–O(1)	2.112(3)
Zn(2)–N(2)	2.153(4)	Zn(2)–O(9)	2.154(3)
Zn(2)–O(5)	2.185(3)	Zn(3)–O(9)	1.921(3)
Zn(3)–O(3)	1.926(3)	Zn(3)–O(2)	1.969(3)
Zn(3)–N(3)	2.104(4)		
Angle	ω, deg	Angle	ω, deg
	I		
O(2)Co(1)O(2)$^{\#1}$	176.45(11)	O(2)Co(1)O(3)	90.02(8)
O(2)$^{\#1}$Co(1)O(3)	89.89(8)	O(3)Co(1)O(3)$^{\#1}$	176.86(12)
O(2)Co(1)N(1)$^{\#2}$	91.78(5)	O(3)Co(1)N(1)$^{\#2}$	91.57(6)
O(2)Co(1)N(2)	88.22(5)	O(3)Co(1)N(2)	88.43(6)
	II		
O(1)Zn(1)O(3)	118.17(17)	O(1)Zn(1)N(2)	100.09(18)
O(3)Zn(1)N(2)	116.61(19)	O(1)Zn(1)N(1)	94.64(18)
O(3)Zn(1)N(1)	107.35(18)	N(2)Zn(1)N(1)	118.27(15)
	III		
O(10)$^{\#1}$Zn(1)O(6)$^{\#1}$	108.26(13)	O(10)$^{\#1}$Zn(1)O(9)	128.54(11)
O(6)$^{\#1}$Zn(1)O(9)	120.50(13)	O(10)$^{\#1}$Zn(1)N(1)	101.15(13)
O(6)$^{\#1}$Zn(1)N(1)	90.55(14)	O(9)Zn(1)N(1)	94.16(12)
O(10)$^{\#1}$Zn(1)O(10)	84.71(11)	O(6)$^{\#1}$Zn(1)O(10)	87.07(12)
O(9)Zn(1)O(10)	82.45(10)	N(1)Zn(1)O(10)	174.12(12)
O(10)Zn(2)O(7)	86.34(12)	O(10)Zn(2)O(1)	175.00(12)
O(7)Zn(2)O(1)	92.33(13)	O(10)Zn(2)N(2)	98.66(12)
O(7)Zn(2)N(2)	91.28(14)	O(1)Zn(2)N(2)	86.19(13)
O(10)Zn(2)O(9)	83.16(10)	O(7)Zn(2)O(9)	91.96(12)
O(1)Zn(2)O(9)	92.07(11)	N(2)Zn(2)O(9)	176.38(13)
O(10)Zn(2)O(5)	93.01(11)	O(7)Zn(2)O(5)	178.44(12)
O(1)Zn(2)O(5)	88.20(13)	N(2)Zn(2)O(5)	90.23(13)
O(9)Zn(2)O(5)	86.55(11)	O(9)Zn(3)O(3)	131.11(14)
O(9)Zn(3)O(2)	108.56(13)	O(3)Zn(3)O(2)	107.16(15)
O(9)Zn(3)N(3)	107.04(13)	O(3)Zn(3)N(3)	97.91(14)
O(2)Zn(3)N(3)	100.58(14)		

* Symmetry transformation used to generate equivalent atoms: $^{\#1} -x+1, y, -z+1/2$; $^{\#2} x, y+1, z$ (**I**); $^{\#1} -x+1, -y+2, -z+1$ (**III**).

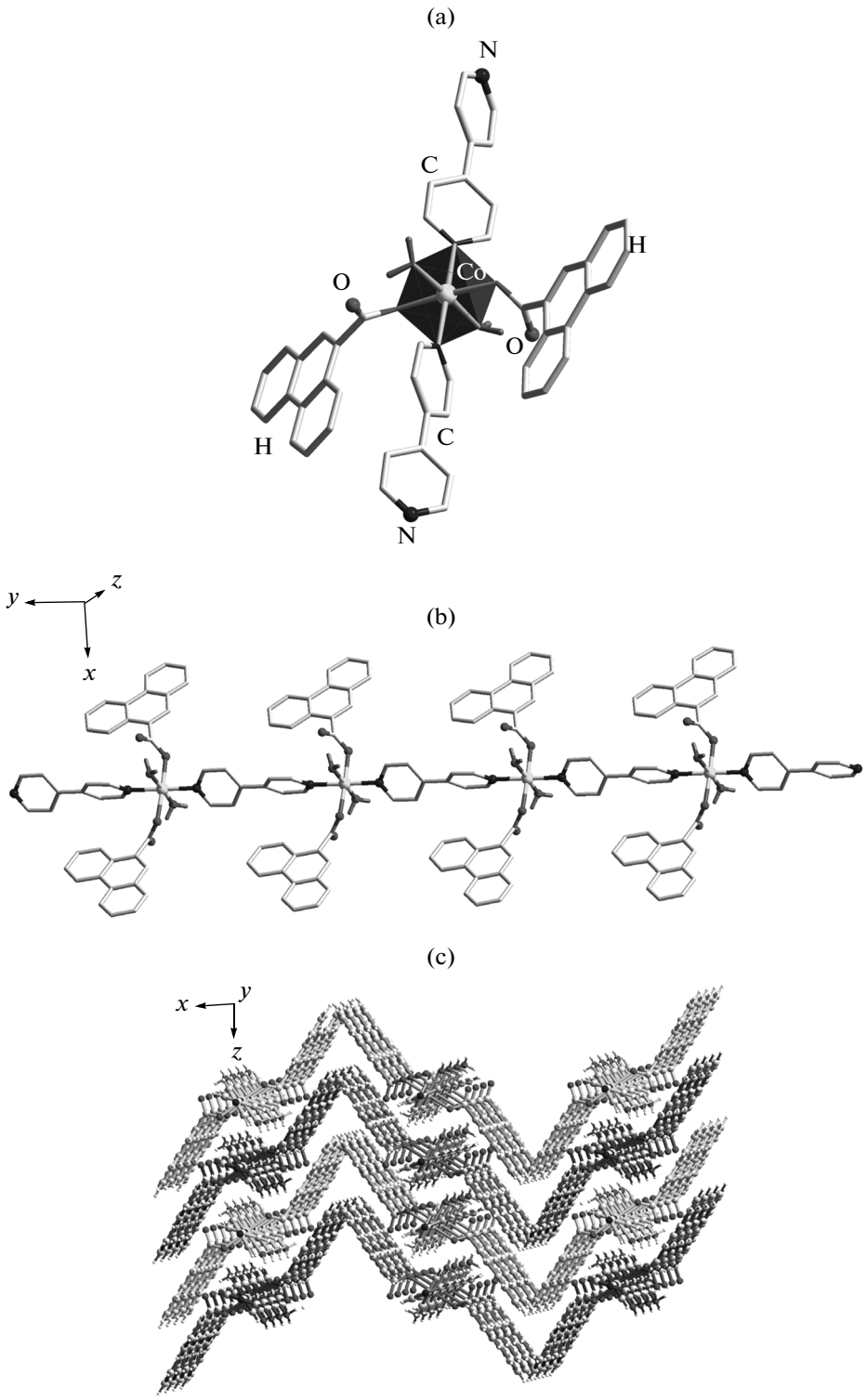

Fig. 1. View of the coordination environment of Co^{2+} ions in **I** (a), 1D linear chain structure in **III** (b); the 3D supramolecular network, formed by the intramolecular O–H···O H-bond and C–H···π interactions in the *y* direction (c). Partial H atoms omitted for clarity.

ligands in bridging coordination mode and two O atoms from two coordinated aqua molecules. The geometry around each Co^{2+} ion can be best described as a distorted octahedron. All the Co–O and Co–N bond lengths, as well as the bond angles around Co(II) center, are in the normal range expected for such coor-

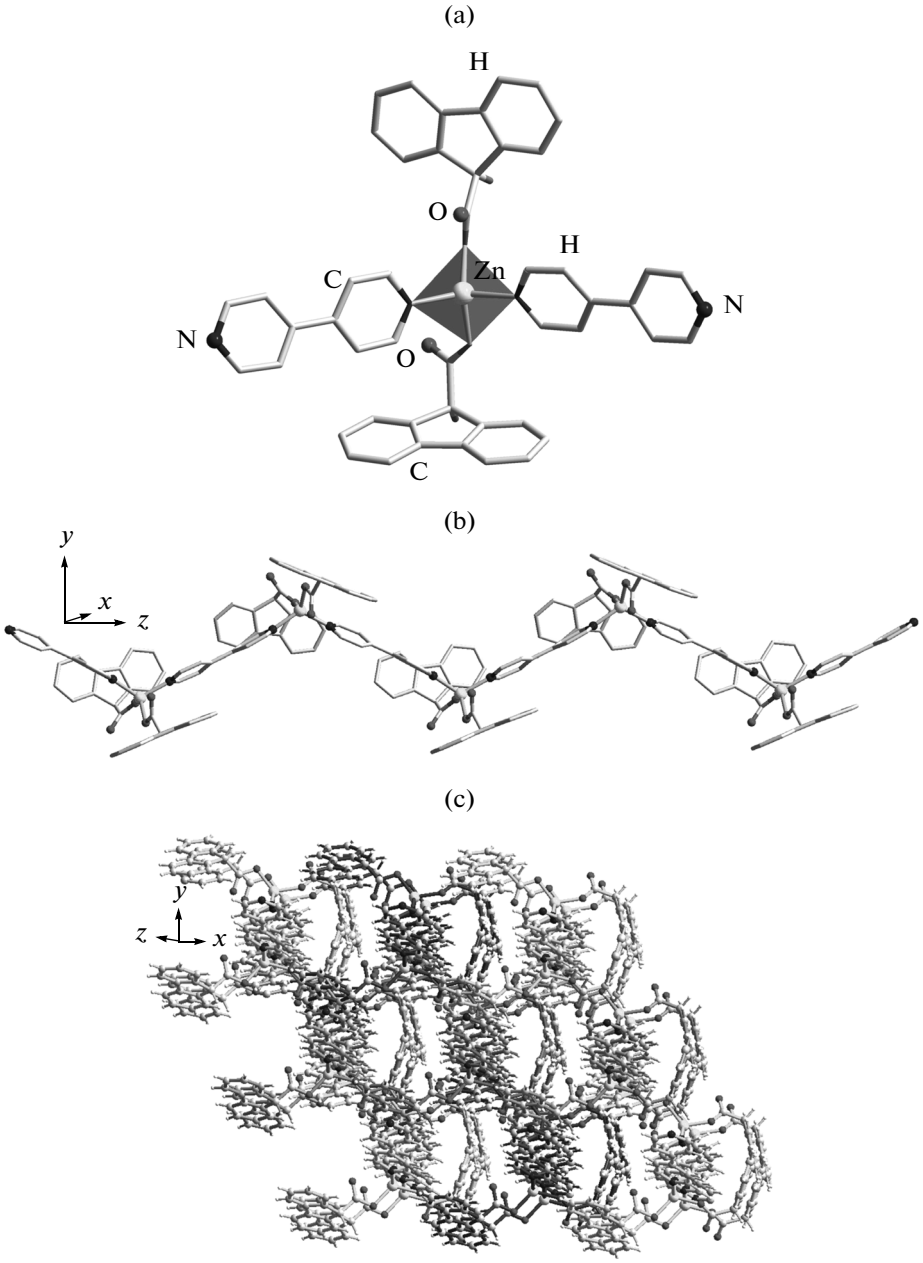

Fig. 2. View of coordination environment of Zn^{2+} ions in **II** (a); 1D zigzag chain structure in **II** (b); the 3D supramolecular framework, formed by the inter-chain C–H···O H-bonding, C–H···π and π···π stacking interactions in the [111] direction (c). Partial H atoms omitted for clarity.

dination compounds (Table 2) [24, 33]. Each Co^{2+} ion is connected to two adjacent Co(II) centers through the 4Bipy bridges to result in a 1D linear chain (Fig. 1b) [34]. Furthermore, the 1D chains are assembled to form a 3D supramolecular network by intermolecular O–H···O (the O(2*w*)···O(3C) separation is 2.772(3) Å and the O(2*w*)–H(2*wB*)···O(3*C*) angle is 171°, symmetry code: (*C*) $-x+1, -y+2, -z$) [35] and C–H···π supramolecular interactions by the edge-to-face orientation between the phenanthrene rings or pyridine and phenanthrene rings (d = 3.792(3), 3.638(3), and 3.675(4) Å, respectively; angle = 161.72(2)°, 130.78(2)°, and 148.31° in the C–H···π patterns) (Fig. 1c) [36, 37].

Although complex **II** is also a 1D structure, different from **I**, each Zn^{2+} ion is four-coordinated by two carboxylate O atoms from two different L^2 ligands in monodentate coordination mode and two N atoms from two different 4bpy molecules to complete a distorted tetrahedral coordination environment, as shown in Fig. 2a. In other words, the Zn^{2+} ion is connected to two adjacent Zn(II) centers through the

4bpy bridges to result in a 1D zigzag chain (Fig. 2b) [38, 39]. They are in good agreement with those reported complexes [40]. In addition, the 1D chains are assembled to form a 3D supramolecular framework by C–H···O H-bonding (the C(17)···O(2*B*) separation is 3.437(2) Å and C(17)–H(17)···O(2*B*) angle is 162°, symmetry code: (*B*) x, $1 - y$, $-0.5 + z$) [35], π···π stacking between pyridine and benzene rings (the centroid-centroid separations are 3.819(8) and 3.687(9) Å, respectively; and the interplanar separations are 3.558(7) and 3.449(7) Å, respectively with the dihedral angle being 13.2° and 9.0°) [41–43]. C–H···π supramolecular interactions by the "edge-to-face" orientation between the benzene rings or pyridine and benzene rings (d = 3.635(2), 3.552(1), 3.742(6), and 3.504(8) Å, respectively; angle = 151.07°, 146.45°, 145.60°, and 165.35° in the C–H···π patterns) [36, 37] (Fig. 2c).

Different from **I** and **II**, OH^- ions of **III** were introduced. X-ray single-crystal diffraction analysis reveals that each asymmetric unit of **III** contains three Zn^{2+} ions, four L^3 ligands, three halves 4Bipy ligands and two μ_3-OH^- ions. As shown in Fig. 3a, there are three kinds of Zn^{2+} ions. Zn(1) ion is five-coordinated by one carboxylate O atom from a L^3 ligand in bidentate bridging coordination mode, one N atom from a 4Bipy molecule and three O atoms from three OH^- ions, respectively, which is in the crystallographical symmetry center with a slightly distorted triangular-bipyramidal coordination geometry. While Zn(2) ion is six-coordinated by two carboxylate O atoms from two L^3 ligands in bidentate bridging coordination mode, one carboxylate O atom from a L^3 ligand in monodentate coordination mode, one N atom from a 4bpy molecule and two O atoms from two OH^- ions to be described as a distorted octahedral coordination environment, and Zn(3) ion is four-coordinated by one carboxylate O atom from a L^3 ligand in bidentate bridging coordination mode, one carboxylate O atom from a L^3 ligand in monodentate coordination mode, one N atom from a 4Bipy molecule and one O atom from a OH^- ion to form a distorted tetrahedral coordination environment. Then, because L^3 ligands have larger steric hindrance, three Zn(II) centers are linked by carboxylate groups of L^3 ligands and OH^- ions to result in a hexanuclear node, which is extended into a 1D linear chain via almost parallelled three 4bpy ligands (Fig. 3b) [34]. All the Zn–N and Zn–O bond distances as well as the bond angles around each Zn(II) center are in the normal range expected for such coordination complexes [40]. It is worth noting that OH^- ions play an important role in the formation of the final structure of **III**. Moreover, the 1D chains are arranged into a 3D supramolecular framework by π···π stacking interactions between pyridine and benzene rings (the centroid-centroid and the interplanar separations are 3.779(5) and 3.456(2) Å, respectively, with the dihedral angle being 5.5°) [41–43] and C–H···π interactions by the edge-to-face orientation between benzene rings (d = 3.781(5) and 3.512(6) Å, respectively; angle = 143.03° and 164.45° in the C–H···π patterns, respectively) [36, 37] (Fig. 3c).

As typical aromatic carboxylic ligands, biphenyl carboxylic acids have been widely used to construct metal-organic coordination architectures. The previously complexes $\{[Cu_2(L^1)_4(Hmta)](H_2O)_{0.75}\}_\infty$ [25], $\{[Cu(FCA)(4Bipy)_{0.5}(4Bipy)_{0.5}](H_2O)(DMF)\}_\infty$ [44] and $[Zn_2(L^3)_4(4Bipy)_2]_\infty$ [45] (Hmta = hexamethylenetetramine, H_2FCA = 9-hydroxy-9*H*-fluorene-9-carboxylic acid and DMF = *N*,*N*-dimethylformamide), were constructed from HL^1, H_2FCA or HL^3, together with 4bpy, showing a 1D zigzag chain with dinuclear Cu(II) nodes, a 2D 4^4 framework and a 1D zigzag chain, respectively. In this research, when 4bpy was used instead of Hmta, we obtained a a 1D linear chain $[Co(L^1)_2(4Bipy)(H_2O)_2]_\infty$ in **I**. And the use of HL^2, whose structures are close to those of H_2FCA, leads to a 1D zigzag chain $[Zn(L^2)_2(4Bipy)_{0.5}(4Bipy)_{0.5}]_\infty$ in **II**. While OH^- anions were introduced, we obtained a 1D linear chain with hexanuclear Zn(II) nodes $[Zn_3(L^3)_4(4Bipy)_{0.5}(4Bipy)_{0.5}(4Bipy)_{0.5}(OH)_2]_\infty$ in **III**. Because ligands all have larger steric hindrance, corresponding complexes show similar 1D chains. However, in partial complexes, because of different metal ions or coordinated OH^- anions, their structures are a little different.

This work also gives a good comparison between three bulky backbone carboxylic acid ligands and corresponding complexes, which indicates that substituent groups of ligands play an important role in the formation of frameworks. Moreover, it should be noticed that metal ions and anions in deeply influenced the final structures.

To confirm that the crystal structures are truly representative of the bulk materials for luminescent and magnetic measurements, XRPD experiments were carried out for the crushed single-crystalline powder samples of **I**–**III**. Because the experimental patterns are almost consistent with those simulated from the single crystal modes, the bulk-synthesized materials and as-grown crystals can still be considered homogeneous.

The solid state luminescent spectrums of **I**–**III** as well as free ligands HL^1, HL^2, HL^3 and 4Bipy were investigated at room temperature (Fig. 4). While the free ligands HL^1, HL^2, HL^3 and 4Bipy display intense luminescence in the solid state at λ_{max} = 391, 345, 339 and 362 nm upon excitation at λ_{ex} = 349/367, 305, 241 and 265 nm, under the same experimental conditions, **I**–**III** exhibit intense purple luminescent emission at λ_{max} = 338, 431 and 402 nm upon excitation at 303, 336 and 323 nm. It is clear that the emission peaks of **I**–**III** are similar to those of the free ligands HL^1, HL^2, HL^3 and 4Bipy. This phenomenon can be tentatively assigned to intraligand transfer π*–π transitions, namely, ligand-to-ligand charge transfer (LLCT), as reported for other complexes [46, 47]. A molecule

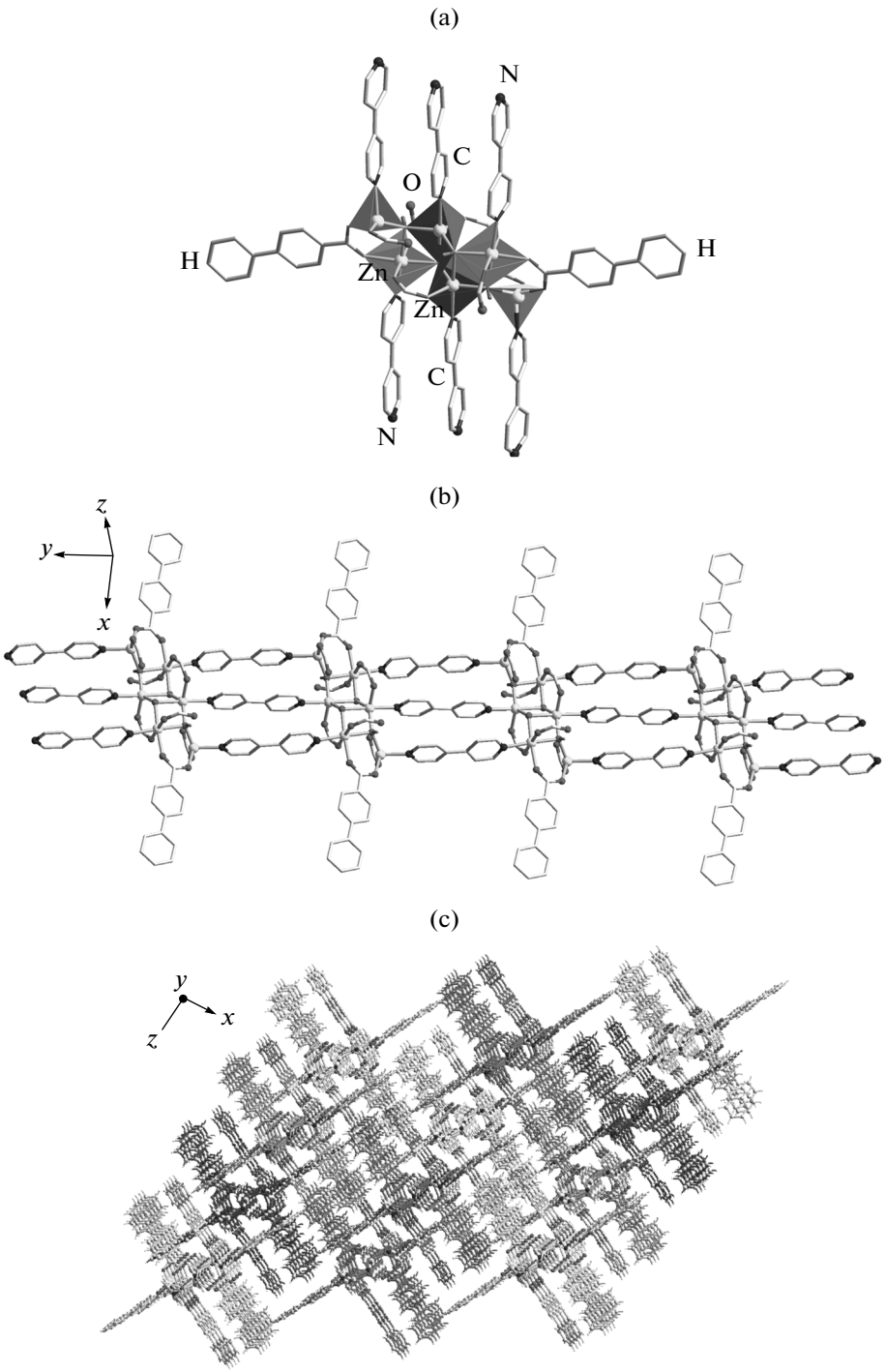

Fig. 3. View of coordination environment of Zn^{2+} ions in **III** (a); 1D linear chain structure in **III** (b); the 3D supramolecular framework, formed by the inter-chain C–H···π and π···π stacking interactions in the *y* direction (c). Partial H atoms and partial substituent groups of L^3 ligands omitted for clarity.

with stronger electronegativity (H_2O) was introduced in **I**, effectively increasing the density of electron cloud in complexes, thereby forming a obvious blue-shift phenomenon compared with the emission of HL^1 [48, 49]. While in **II** and **III**, an obvious red shift relative to that of the free ligands HL^2, HL^3 and 4Bipy, which may originate from the strong conjugation and intermolecular interaction between the molecule segments of ligands [50, 51]. Moreover, the different relative intensity among **I**–**III** might be assigned to the structural diversity along with a different ratio of HL^1, HL^2 or HL^3 ligands, or to 4Bipy in the complexes, or the

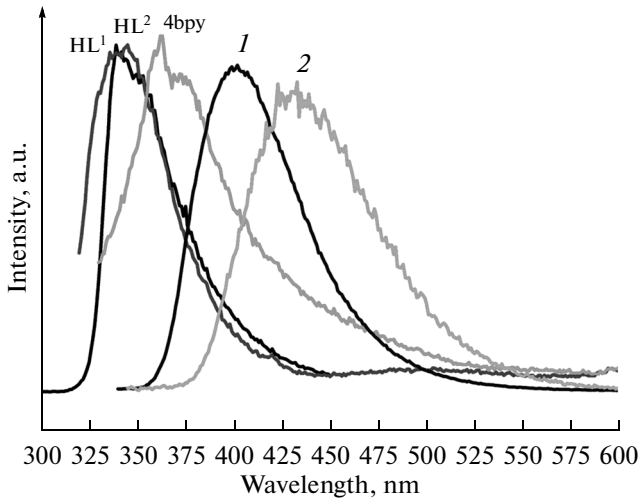

Fig. 4. Solid emission spectra of HL^1, HL^2, 4Bipy and **I**, **II** at room temperature (λ_{ex} = 368, 304, 315 nm for HL^1, HL^2, 4Bipy and 303, 336 nm for **I**, **II**, respectively).

strong conjugation and inter/intramolecular interaction between the molecule segments of ligands [22].

ACKNOWLEDGMENTS

This work was supported by the key project of Science and Technology Department of Henan Province (no. 112102210371) and the key project of education Department of Henan Province (no. 12B150003).

REFERENCES

1. Lu, Z.Z., Zhang, R., Li, Y.Z., et al., *J. Am. Chem. Soc.,* 2011, vol. 133, p. 4172.
2. Das, M.C., Xiang, S.C., Zhang, Z.J., et al., *Angew. Chem. Int. Ed.*, 2011, vol. 50, p. 10510.
3. Sumida, K., Rogow, D.L., Mason, J.A., et al., *Chem. Rev.*, 2012, vol. 112, p. 724.
4. Cook, T.R., Zheng, Y.R., and Stang, P.J., *Chem. Rev.*, 2013, vol. 113, p. 734.
5. Mal, P., Schultz, D., Beyeh, K., et al., *Angew. Chem. Int. Ed.*, 2008, vol. 47, p. 8297.
6. Su, Z., Chen, S.S., Fan, J., et al., *Cryst. Growth Des.*, 2010, vol. 10, p. 3675.
7. Liu, X., Oh, M., and Lah, M.S., *Inorg. Chem.*, 2011, vol. 50, p. 5044.
8. Li, Y.W., Ma, H., Chen, Y.Q., et al., *Cryst. Growth Des.*, 2012, vol. 12, p. 189.
9. Eddaoudi, M., Kim, J., Rosi, N., et al., *Science*, 2002, vol. 295, p. 469.
10. Yang, J., Li, B., Ma, J.F., et al., *Chem. Commun.*, 2010, vol. 46, p. 8383.
11. Zhang, J., Bu, J.T., Chen, S., et al., *Angew. Chem. Int. Ed.*, 2010, vol. 49, p. 8876.
12. Higuchi, M., Nakamura, K., Horike, S., et al., *Angew. Chem. Int. Ed.,* 2012, vol. 51, p. 8369.
13. Meng, Z.R., He, X., Wu, X.Y., et al., *Chin. J. Struct. Chem.*, 2006, vol. 25, p. 1293.
14. Serre, C., Mellot-Draznieks, C., Surble, S., et al., *Science*, 2007, vol. 315, p. 1828.
15. Li, X.H., Fang, M., and Zhao, B., *Sci. China, B*, 2009, vol. 52, p. 1456.
16. Gong, H.Y., Rambo, B.M., Karnas, E., et al., *J. Am. Chem. Soc.*, 2011, vol. 133, p. 1526.
17. Medishetty, R., Koh, L.L., Kole, G.K., et al., *Angew. Chem. Int. Ed.,* 2011, vol. 50, p. 10949.
18. Nagarkar, S.S., Chaudhari, A.K., and Ghosh, S.K., *Inorg. Chem.*, 2012, vol. 51, p. 572.
19. Hirai, K., Furukawa, S., Kondo, M., et al., *Angew. Chem. Int. Ed.*, 2011, vol. 50, p. 8057.
20. Gao, Q., Xie, Y.B., Li, J.R., et al., *Cryst. Growth Des.,* 2012, vol. 12, p. 281.
21. Wang, J.J., Hu, T.L., and Bu, X.H., *CrystEngComm*, 2011, vol. 13, p. 5152.
22. Chang, Z., Zhang, A.S., Hu, T.L., et al., *Cryst. Growth Des.*, 2009, vol. 9, p. 4840.
23. Lu, Y.B., Wang, M.S., Zhou, W.W., et al., *Inorg. Chem.*, 2008, vol. 47, p. 8935.
24. Liu, C.S., Wang, J.J., Yan, L.F., et al., *Inorg. Chem.*, 2007, vol. 46, p. 6299.
25. Wang, J.J., Chang, Z., Zhang, A.S., et al., *Inorg. Chim. Acta,* 2010, vol. 363, p. 1377.
26. Bu, X.H., Wang, J.J., Liu, C.S., et al., *Patent-Faming Zhuanli Shenqing Gongkai Shuomingshu*, 2007, Pat. no. CN 101016243 A 20070815; Application no. CN 2006-1001608520060930.
27. *SAINT, Software Reference Manual*, Madison (WI, USA): Bruker AXS, 1998.
28. Sheldrick, G.M., *SADABS, Siemens Area Detector Absorption Corrected Software*, Göttingen (Germany): Univ. of Göttingen, 1996.
29. Sheldrick, G.M., *SHELXTL NT, Version 5.1, Program for Solution and Refinement of Crystal Structures,* Göttingen (Germany): Univ. of Göttingen, 1997.
30. *Comprehensive Coordination Chemistry*, Wilkinson, G., Gillard, R.D., and McCleverty J.A., Eds., Oxford: Pergamon, 1987, vol. 5.
31. Nakamoto, K., *Infrared and Raman Spectra of Inorganic and Donor Hydrogen Bond Coordination Compounds*, New York: Wiley, 1986.
32. Deacon, G.B. and Phillips, R.J., *Coord. Chem. Rev.*, 1980, vol. 33, p. 227.
33. Wang, J.J., Zhang, Y.J., Chen, J., et al., *Inorg. Chim. Acta*, 2014, vol. 411, p. 30.
34. Liu, S.J., Zhao, J.P., Song, W.C., et al., *Inorg. Chem.*, 2013, vol. 52, p. 2103.
35. Desiraju, G.R. and Steiner, T., *The Hydrogen Bond in Structural Chemistry and Biology*, Oxford: Oxford Univ., 1999.
36. Abernethy, C.D., Macdonald, C.L.B., Cowley, A.H., et al., *Chem. Commun.*, 2001, p. 61.
37. Sony, S.M.M. and Ponnuswamy, M.N., *Cryst. Growth Des.*, 2006, vol. 6, p. 736.
38. Wang, Y., He, C.T., Liu, Y.J., et al., *Inorg. Chem.*, 2012, vol. 51, p. 4772.

39. Wang, X., Luan, J., Sui, F., et al., *Cryst. Growth Des.*, 2013, vol. 13, p. 3561.
40. Wang, J.J., Liu, C.S., Hu, T.L., et al., *CrystEngComm*, 2008, vol. 10, p. 681.
41. Janiak, C., *Dalton Trans.*, 2000, p. 3885.
42. Khlobystov, A.N., Blake, A.J., Champness, N.R., et al., *Coord. Chem. Rev.*, 2001, vol. 222, p. 155.
43. Hobza, P. and Havlas, Z., *Chem. Rev.*, 2000, vol. 100, p. 4253.
44. Liu, S.X., *Acta Crystallogr., Secr. C: Cryst. Struct. Commun.*, 1992, vol. 48, p. 22.
45. Burrows, A.D., Mahon, M.F., Raithby, P.R., et al., *CrystEngComm*, 2012, vol. 14, p. 3658.
46. Bo, Q.B., Wang, H.Y., Wang, D.Q., et al., *Inorg. Chem.*, 2011, vol. 50, p. 10163.
47. Miyasaka, H., *Acc. Chem. Res.*, 2013, vol. 46, p. 248.
48. Abuelela, A.M., Mohamed, T.A., and Prezhdo, O.V., *J. Phys. Chem., C,* 2012, vol. 116, p. 14674.
49. Chen, J.G., Liu, X., Liu, Z.W., et al., *Macromolecules*, 2012, vol. 45, p. 4907.
50. Wu, P., He, C., Wang, J., et al., *J. Am. Chem. Soc.*, 2012, vol. 134, p. 14991.
51. Demel, J., Kubát, P., Millange, F., et al., *Inorg. Chem.*, 2013, vol. 52, p. 2779.